DOI: 10.1002/chem.200800628

A Combined Experimental and Theoretical Study of the Molecular Inclusion of Organometallic Sandwich Complexes in a Cavitand Receptor

Erik Zuidema,[a] M. Angeles Sarmentero,[a] Carles Bo,*[a] and Pablo Ballester*[a, b]

Abstract: We describe herein a detailed study of the inclusion processes of several positively charged organometallic sandwich complexes inside the aromatic cavity of the self-folding octaamide cavitand **1**. In all cases, the binding process produces aggregates with a simple 1:1 stoichiometry. The resulting inclusion complexes are not only thermodynamically stable, but also kinetically stable on the ^{1}H NMR spectroscopy timescale. The binding constants for the inclusion complexes were determined by different titration techniques. We have also investigated the kinetics of the binding process and the motion of the metallocenes included in the aromatic cavity of the host. Using DFT-based calculations, we have evaluated the energies of a diverse range of potential binding geometries for the complexes. We then computed the proton chemical shifts of the included guest in each one of the binding geometries. The agreement between the averaged computed values and the experimentally determined chemical shifts clearly supports the proposed binding geometries that we assigned to the inclusion complexes formed in solution. The combination of experimental and theoretical results has allowed us to elucidate the origins of the distinct features detected in the complexation process of the different guests, as well as their different motions inside the host.

Keywords: cavitands · density functional calculations · host–guest systems · metallocenes · supramolecular chemistry

Introduction

The use of unimolecular vessels and supramolecular assemblies to include or encapsulate transition-metal complexes has received considerable attention over the last two decades. Numerous examples have been reported in which noncovalent confinement of the transition-metal guest in the interior of the receptor's cavity led to changes in its chemical behavior. Early studies mainly focused on the effects of inclusion on the redox properties of stable metallocene complexes.[1] More recently, the possibility of stabilizing reactive organometallic species by encapsulating them inside multicomponent supramolecular architectures has been demonstrated.[2] Furthermore, the first examples of catalysis using transition-metal complexes that are encapsulated inside supramolecular assemblies have been reported in which encapsulation of the catalyst leads to significant changes in catalyst stability, activity, and/or selectivity.[2,3]

Resorcinarene-based cavitands have been shown to be selective unimolecular receptors for a variety of organic species of appropriate size.[4] They bind cationic guests through cation–π and CH–π interactions and consequently they have been successfully applied as organocatalysts in reactions that involve positively charged intermediates and/or products.[5] The discrete 1:1 stoichiometry of the host–guest complexes often obtained with these unimolecular receptors greatly facilitate an in-depth study of the structure of the formed inclusion complexes and their dynamic behavior by spectroscopic techniques.[2a,6]

Recently, some of us showed that three-walled hybrid cavitand resorcin[4]arenes **3a** and **3b** are not only able to include organic ammonium cations (Scheme 1),[7] but also similarly sized cationic transition-metal sandwich complexes, which lead to the formation of thermodynamically and kinetically stable 1:1 host–metallocenium complexes in nonaqueous media.[8] Fast spinning and tumbling of the sandwich complex inside the three-walled host and a slow ex-

[a] Dr. E. Zuidema, Dr. M. A. Sarmentero, Dr. C. Bo, Prof. P. Ballester
The Institute of Chemical Research of Catalonia (ICIQ)
Avda. Països Catalans, 16, 43007 Tarragona (Spain)
Fax: (+34) 977-920-221
E-mail: cbo@iciq.es
pballester@iciq.es

[b] Prof. P. Ballester
Catalan Institution for Research and Advanced Studies (ICREA)
Pg. Lluis Companys, 23, 08010 Barcelona (Spain)

Supporting information for this article is available on the WWW under http://www.chemeurj.org/ or from the author.

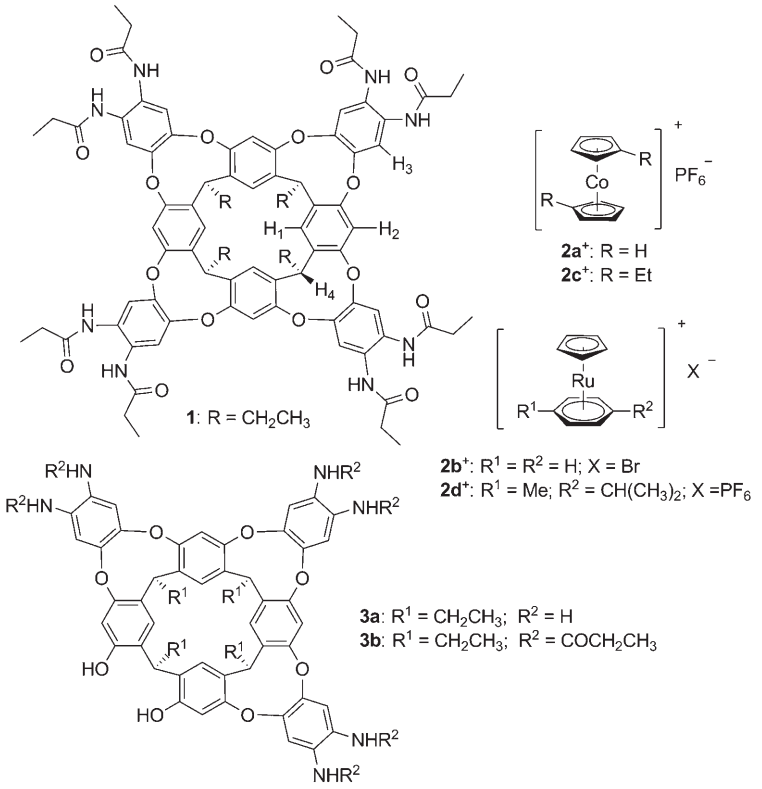

Scheme 1. Molecular structures of the receptors **1**, **3a, 3b**, and the cationic sandwich complexes $\mathbf{2a}^+$–$\mathbf{2d}^+$.

change between the free and bound guest on the ^{1}H NMR spectroscopy timescale were observed. Also, the electron-rich microenvironment found in the interior of the host's cavity hampered the reduction of the included transition-metal complex, presumably by stabilizing the (oxidized) cationic species.

In comparison with the scoop-shaped, three-walled hybrid cavitand resorcin[4]arene **3b**, bowl-shaped native resorcin[4]arene-based cavitand **1** provides a more enclosed cavity and therefore creates a more effective microenvironment for guest-binding.[9] In addition, the steric requirements dictated by the deep vase of cavitand **1** are very different from those of the open structure of the three-walled cavitand **3b**, imposing different constraints on the rotational motion of the guest inside the host as well as affecting the exchange processes of the included guest. Clearly, an in-depth understanding of the structures and dynamic behavior of the inclusion complexes formed by transition-metal guests and four-walled cavitand **1** is of key importance for the development of potential supramolecular catalysts derived from complexes of this nature.

Herein we present a detailed study of the inclusion process of sandwich complexes $\mathbf{2a}^+$–$\mathbf{2d}^+$ inside four-walled resorcin[4]arene-based host **1** (Scheme 1). The structures and dynamic behavior of the guest inside the host, as well as the exchange processes involving the included guest, have been studied by different NMR spectroscopic techniques. Isothermal titration calorimetry (ITC) experiments were also performed to determine the thermodynamic parameters of the inclusion process of $\mathbf{2a}^+$. In addition, the structural features of the complexes formed by the inclusion of metallocenes **2** in the deep aromatic cavity of receptor **1** were studied by DFT-based calculations. The calculated ^{1}H NMR chemical shifts of the included guests are in good agreement with the experimentally determined values. Comparison of the theoretical and experimental results has provided an insight into the relationship between the shape and size of the different guests $\mathbf{2a}^+$–$\mathbf{2d}^+$ and their inclusion geometry. Furthermore, the results derived from variable-temperature (VT) ^{1}H NMR studies and exchange spectroscopy (EXSY) experiments carried out on the complexes demonstrate the existence of distinct dynamic behavior in the motion of the different guests within **1**.

Results and Discussion

Unsubstituted metallocene guests: The binding of octaamide cavitand **1** to cobaltocenium $\mathbf{2a}^+\cdot PF_6^-$ and ruthenocenium $\mathbf{2b}^+\cdot Br^-$ was probed by ^{1}H NMR titration techniques. In the absence of a guest, the ^{1}H NMR spectra of **1** in [D_6]acetone showed sharp signals for all the aromatic and methine protons, which indicates that host **1** adopts a vase conformation that is stabilized by an array of intramolecular hydrogen bonds established between the amide residues along the upper rim of the cavitand.[9] The hydrogen bonds formed by the amides of cavitand **1** result in two cycloenantiomers, with clockwise or counterclockwise orientation.[9b] The ^{1}H NMR spectrum showed just one broad singlet at $\delta =$ 9.5 ppm, which has been assigned to the eight NH protons of **1** (Figure 1). This observation is indicative of a fast interconversion between the two enantiomers on the ^{1}H NMR spectroscopy timescale in [D_6]acetone and at room temperature.

Two different sets of signals corresponding to the NH groups and aromatic protons of the free and bound host **1** were observed during the initial additions of the cationic guest $\mathbf{2a}^+$ or $\mathbf{2b}^+$ to a [D_6]acetone solution containing cavitand **1** (Figure 1). In addition, during the titration with cobaltocenium $\mathbf{2a}^+$, two sharp singlets resonating at $\delta = 3.4$ and 6.0 ppm were also detected. These two singlets were assigned to the protons of included and free $\mathbf{2a}^+$, respectively.

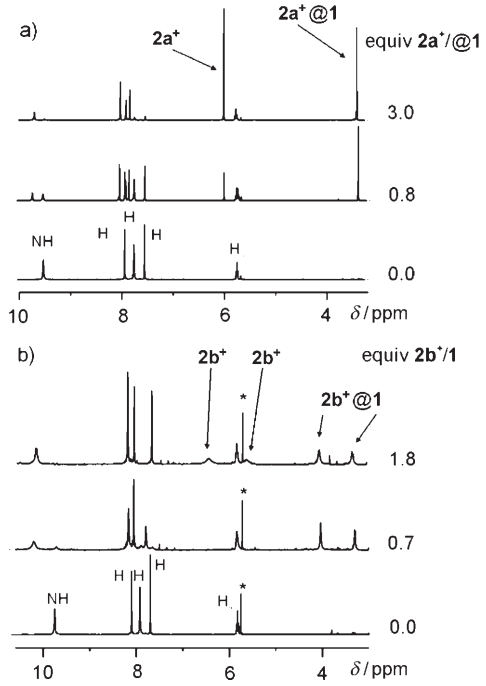

Figure 1. Changes in the ^{1}H NMR (500 MHz, [D$_6$]acetone) spectra acquired at 298 K during a) the titration of **1** with **2a**$^+$ ([**1**] = 1.03 mM) and b) the titration of **1** with **2b**$^+$ ([**1**] = 2.90 mM). * indicates residual CH_2Cl_2.

Note that the cyclopentadienyl protons of the included **2a**$^+$ appear as a single sharp singlet. For the ruthenocenium guest **2b**$^+$, two separate signals are observed for the protons of the cyclopentadienyl and benzene ligands for both the free and bound guest. The large upfield shifts observed for the proton resonances of **2a**$^+$ ($\Delta\delta = -2.6$ ppm) and **2b**$^+$ ($\Delta\delta = -2.4$ ppm for the C_6H_6 moiety and $\Delta\delta = -2.3$ ppm for the C_5H_5 moiety of the guest) upon binding to host **1** have been attributed to the magnetic shielding microenvironment experienced by the guest when included within the four aromatic rings of **1**. The observation of two different sets of proton signals for free and bound **2a**$^+$ and **2b**$^+$, as well as for free and bound host **1** are indicative of the formation of host–guest complexes that are kinetically stable on the ^{1}H NMR spectroscopy timescale. The observation of just one sharp singlet for the 10 cyclopentadienyl protons of included **2a**$^+$ and of only two types of resonances with similar upfield shifts for bound **2b**$^+$ suggest that at 298 K guests **2a**$^+$ and **2b**$^+$ spin and tumble rapidly within **1**. VT ^{1}H NMR experiments indicated that even at temperatures as low as 200 K, the motions experienced by the included guests inside **1** remain fast on the ^{1}H NMR spectroscopy timescale. The motion of the included guests controls the interconversion between the different binding geometries that could be adopted in the inclusion complexes (see below).

It was possible to calculate the association constants for the inclusion complexes **2a**$^+$**@1** and **2b**$^+$**@1** in [D$_6$]acetone (Table 1) from the ^{1}H NMR titration experiments. For complex **2a**$^+$**@1**, an association constant of $K_a = (7.0 \pm 0.7) \times 10^3\,\text{M}^{-1}$ was determined from the relative areas of the aromatic proton signals of the free and bound host **1**. A similar value was obtained when the areas of the proton signals of the free and bound guest **2a**$^+$ were used. In the case of **2b**$^+$**@1**, an association constant of $K_a = (6.2 \pm 1.5) \times 10^3\,\text{M}^{-1}$ was determined from the areas of the proton signals assigned to the amide moieties of the free and bound cavitand **1**.

Table 1. Binding constants for the cationic metallocene sandwich complexes formed with receptor **1** in acetone.

Metallocene	K_a [$10^3\,\text{M}^{-1}$]
2a$^+$·PF_6^-	7.0 ± 0.7[a]/6.9 ± 0.4[b]
2b$^+$·Br^-	6.2 ± 1.5[a]
2c$^+$·PF_6^-	0.12 ± 0.04[a]
2d$^+$·PF_6^-	0.08 ± 0.01[a]

[a] Determined by ^{1}H NMR titration. [b] Determined by ITC titration.

The thermodynamics of the binding of cobaltocenium **2a**$^+$ with receptor **1** in acetone was investigated by ITC. The calorimetric titration was carried out by the sequential injection of a solution of guest **2a**$^+$ ([**2a**$^+$] = 49.40 mM) in acetone into a solution of cavitand **1** ([**1**] = 6.60 mM) in acetone maintained at 25 °C. Figure 2 shows the normalized integration data for the heat (exothermic) evolved per injection (in kcal mol^{-1}) of injectant (**2a**$^+$) plotted against the molar ratio [**2a**$^+$]/[**1**]. The binding isotherm is sigmoidal and shows an inflection point at 1.0, which indicates a 1:1 stoichiometry for the complex being formed (**2a**$^+$**@1**). The heat of binding was fitted to a 1:1 module binding algorithm, which yielded an association constant of $K_a = (6.9 \pm 0.4) \times 10^3\,\text{M}^{-1}$, in good agreement with the association constant obtained by NMR spectroscopy. The thermodynamic parameters show a moderate enthalpic ($\Delta H = (-3.12 \pm 0.01)$ kcal mol^{-1}) and a favorable entropic ($T\Delta S = 2.12$ kcal mol^{-1}) contribution to the free energy of association. The entropic gain was attributed to the release of ordered acetone molecules from the surface of free species upon formation of the complex, which causes a net increase in disorder for the overall system (desolvation + binding). The enthalpic gain of binding is due to

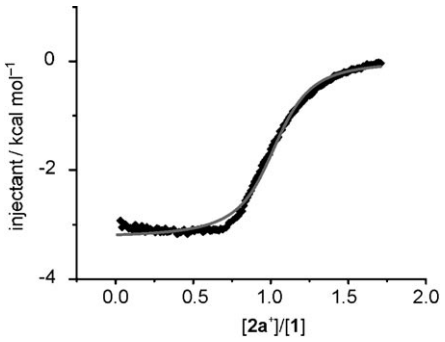

Figure 2. ITC titration of the formation of the **2a**$^+$**@1** complex. The normalized integration data of the evolved heat per injection (in kcal mol^{-1}) of injectant (**2a**$^+$) plotted against the molar ratio [**2a**$^+$]/[**1**]. To determine the values of the thermodynamic variables (ΔH, ΔG, and $T\Delta S$), the ITC data were fitted to a 1:1 binding model (line). $n = 1.07 \pm 0.00489$, $K_a = (6.91 \pm 0.4) \times 103\,\text{M}$, $\Delta H = (-3122 \pm 15.42)$ cal mol^{-1}, $T\Delta S = 2120$ cal mol^{-1}.

the fact that the cation–π interactions established between the receptor and the bound guest are more favorable than the cation–dipole interactions between the acetone molecules of the solvent and the free guest.

The kinetics of the complexation of $\mathbf{2a}^+$ by **1** at 298 K were investigated by EXSY spectroscopy (see the Supporting Information). 2D EXSY[10] is a relatively simple and direct NMR method for studying the kinetics of reversible systems that exchange slowly on the ^{1}H NMR spectroscopy timescale. By this technique, we measured a rate constant ($k_{-1}=0.15\ s^{-1}$) that corresponds to a chemical exchange barrier, $\Delta G^{\neq}_{diss}$, of 18.70 kcal mol^{-1} for the guest exiting the host. The barrier of self-exchange depends not only on the energy required for the host to reorganize to a conformation that can release the guest, but also on the nature of the guest, which in turn, is responsible for the thermodynamic stability of the complex. The free energy for the formation of the $\mathbf{2a}^+$@**1** complex, calculated from the stability constant reported in Table 1, is $\Delta G_{\mathbf{2a}+@\mathbf{1}}=-5.24$ kcal mol^{-1}. Accordingly, we can estimate the barrier for the reorganization of the host during the dissociation of the hybrid–cavitand complex to be $\Delta G^{\neq}_{conf}=\Delta G^{\neq}_{diss}-\Delta G_{\mathbf{2a}+@\mathbf{1}}=13.46$ kcal mol^{-1}. The high value estimated for the free energy barrier for the host to reorganize to a conformation that can release the guest in acetone hints at an exchange process that requires the four walls of the vase conformer to unfold into the kite conformer.[11]

The low-energy geometries of the inclusion complexes of $\mathbf{2a}^+$ and $\mathbf{2b}^+$ with host **1** were investigated by DFT-based calculations. The optimized structures, relative energies, and calculated ^{1}H NMR chemical shifts of the different coordination modes of guests $\mathbf{2a}^+$ and $\mathbf{2b}^+$ in host **1** are shown in Figure 3. For both guests $\mathbf{2a}^+$ and $\mathbf{2b}^+$, the included cationic metallocene preferentially adopts an axial or pseudoaxial conformation inside host **1**.[12] For ruthenium-based metallocene $\mathbf{2b}^+$, there is little energetic preference for either of the two different axial orientations of this asymmetric guest inside host **1**. This is consistent with the similar values observed for the upfield shifts of the ^{1}H NMR signals of both the cyclopentadienyl and benzene hydrogen atoms of guest $\mathbf{2b}^+$ upon inclusion in the deep aromatic cavity of host **1** (Figure 1b).

For complexes $\mathbf{2a}^+$@**1** and $\mathbf{2b}^+$@**1** the equatorial inclusion geometry is less favorable than the pseudoaxial inclusion geometry. The larger energy difference between the equatorial and axial geometries computed for $\mathbf{2b}^+$ relative to $\mathbf{2a}^+$ is readily explained by the larger arene–arene distance in the ruthenium-based metallocene $\mathbf{2b}^+$ relative to cobaltocenium $\mathbf{2a}^+$. For both guests, however, the relative energy of the equatorial geometry is not prohibitively high so as to prevent the tumbling of the guest inside the host that is observed experimentally. Furthermore, the fact that the molecular structures of the host in the two different complex geometries are very similar indicates that any reorientation of the guest inside the host does not require significant deformation of the host cavity.

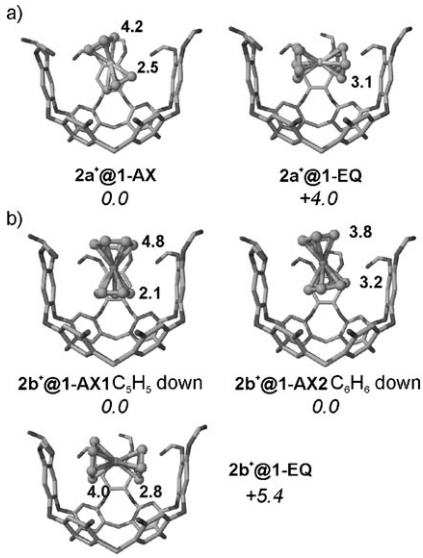

Figure 3. Optimized binding geometries for the inclusion complexes: a) Cobaltocenium guest $\mathbf{2a}^+$ in modified host **1**. Left: Pseudoaxial geometry; right: equatorial geometry. b) Ruthenocenium guest $\mathbf{2b}^+$ in modified host **1**. Top Left: Axial geometry with the Cp ligand down; top right: axial geometry with Cp ligand up; bottom left: equatorial geometry. All of the hydrogen atoms and one wall of the cavitand have been removed for clarity. The calculated chemical shifts of the guest protons inside the host, relative to TMS, are shown in bold. Values in italics beneath each structure denote the relative energy of each binding geometry in kcal mol^{-1}.

Because it is clear from the ^{1}H NMR spectroscopy experiments described above that the different low-energy geometries computed for the inclusion complexes $\mathbf{2a}^+$@**1** and $\mathbf{2b}^+$@**1** are involved in a fast chemical exchange on the ^{1}H NMR spectroscopy timescale due to the spinning and tumbling motion of the guest inside the host, we calculated the Boltzmann-weighted average chemical shifts for the ^{1}H NMR signals of guests $\mathbf{2a}^+$ and $\mathbf{2b}^+$ inside host **1** at 298 K based on the relative energies of the different structures reported in Figure 3. For cobaltocenium $\mathbf{2a}^+$, this yielded an averaged chemical shift value of $\delta=3.4$ ppm for all 10 protons of the two cyclopentadienyl moieties, which reproduces very nicely the experimentally measured value of $\delta=3.4$ ppm (Figure 1a). Also, for the included ruthenium guest $\mathbf{2b}^+$, the averaged chemical shifts of $\delta=4.0$ ppm calculated for the benzene protons and $\delta=3.2$ ppm for the cyclopentadienyl protons of the guest are in excellent agreement with the experimental values ($\delta=4.0$ and 3.3 ppm, respectively, Figure 1b).

Owing to the high thermodynamic stability constant of the $\mathbf{2a}^+$@**1** complex, we were also able to study its electrochemical properties in acetone by cyclic voltammetry (Figure 4). We observed that the inclusion of $\mathbf{2a}^+$ inside the cavitand affects its half-wave redox potential, with $E_{1/2}$ shifting approximately 86 mV to a more negative potential. This indicates that the inclusion complex formed with the cationic $\mathbf{2a}^+$ species inside cavitand **1** is more stable thermodynamically than the corresponding complex formed with the neutral reduced metallocene (cobaltocene).[1c,13] The shift of

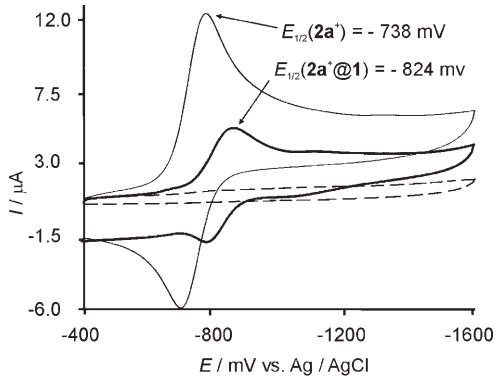

Figure 4. Voltammetric response on glass carbon (0.071 cm^2) of a 1.0 mM solution of **1** containing 0.1 M tetraoctylammonium bromide in the absence of $\mathbf{2a}^+$ (-----) and in the presence of 0.4 equiv of $\mathbf{2a}^+$ (——). The CV of a 0.4 mM solution of $\mathbf{2a}^+$ containing 0.1 M tetraoctylammonium bromide is also shown for comparison (——).

the half-wave potential for $\mathbf{2a}^+$ upon inclusion in **1** was used to calculate the stability constant of the inclusion complex of the neutral cobaltocene. We obtained a stability constant for the neutral metallocene of $K_{\mathbf{2a@1}} = 2.5 \times 10^2\,M^{-1}$ (by using $K_{\mathbf{2a+@1}} = 7.0 \times 10^3\,M^{-1}$, obtained from the ^{1}H NMR spectroscopy experiments).[14] Schaefer III and co-workers previously studied the structure and molecular orbitals of neutral cobaltocene in the gas phase by DFT-based calculations and compared them with the results of calculations performed on neutral ferrocene, which is isoelectronic with the cationic guest $\mathbf{2a}^+$.[15] They showed that the additional electron in cobaltocene leads to a Jahn–Teller effect that distorts the metallocene structure from D_{5d} to C_{2v} symmetry by shortening the distance between the metal and one carbon atom in each cyclopentadienyl ligand. The geometric distortion is very small, however, and consequently the lower stability constant $K_{\mathbf{2a@1}}$ observed for the inclusion complex of neutral cobaltocene cannot be attributed to geometric constraints imposed by host **1**. The difference in the stability constants for guest $\mathbf{2a}^+$**@1** and its reduced form **2a@1** is clearly due to the loss of the cation–π contribution to the overall host–guest binding interaction upon reduction of the bound guest $\mathbf{2a}^+$.

Because the changes in the geometry of $\mathbf{2a}^+$ upon reduction are small, the energies of empty guest-based orbitals of free $\mathbf{2a}^+$ and encapsulated $\mathbf{2a}^+$**@1**, obtained from DFT-based calculations, can be used to investigate the effect of inclusion on the redox potential of the guest. For both free $\mathbf{2a}^+$ and encapsulated $\mathbf{2a}^+$**@1**, the calculations predict that the lowest unoccupied molecular orbital (LUMO) is a well-localized metal-based d orbital. Most likely, this will be the orbital involved in the reduction process. The calculated orbital energies of the LUMOs of free and encapsulated $\mathbf{2a}^+$ are reported in Table 2. The orbital energies of the cationic guest $\mathbf{2a}^+$ are highly solvent-dependent, especially in the absence of host **1**. Therefore, solvent effects on the gas-phase optimized structures were included by an implicit solvation model for two different solvents (Table 2).

Table 2. Calculated energies of the lowest unoccupied molecular orbital (LUMO) of $\mathbf{2a}^+$ in the absence of host **1** and included in host **1** in the gas phase, cyclohexane, and water.

Solvent	E [eV]		
	$\mathbf{2a}^+$	$\mathbf{2a}^+$**@1-ax**	$\mathbf{2a}^+$**@1-eq**
–	−6.36	−5.14	−5.12
cyclohexane	−4.34	−4.01	−3.97
water	−2.39	−2.73	−2.59

As expected, the effect of solvation on the orbital energies of free $\mathbf{2a}^+$ is pronounced. In comparison, solvation effects are smaller for $\mathbf{2a}^+$**@1**. As has been suggested previously, the host acts as a polar microenvironment that partially isolates the encapsulated guest from the bulk solvent. The π interior surface of the cavitand host is highly electron-rich, and this enhances the electron density of the included metal center of the guest. This in turn leads to an increase in the orbital energies of the guest. Both in the gas phase and in the nonpolar cyclohexane solvent, higher LUMO energies for the encapsulated guest than the free solvated guest were predicted. This is consistent with the experimental observation that the guest is more difficult to reduce inside cavitand **1**.

1,1′-Diethyl-substituted cobaltocenium guest $\mathbf{2c}^+$: The stability constant of complex $\mathbf{2c}^+$**@1**, determined from the relative areas of the proton signals of free and bound **1** in ^{1}H NMR titration experiments, is one order of magnitude lower than that of complex $\mathbf{2a}^+$**@1** (Table 1). At room temperature and after the addition of $\mathbf{2c}^+$ (1.5 equiv) to a solution of **1** in [D_6]acetone, separate proton signals were observed for free and bound host **1**, as well as for guest $\mathbf{2c}^+$. This observation is again indicative of the existence of a slow chemical exchange on the ^{1}H NMR spectroscopy timescale between the free and bound states of the host and guest and the formation of a kinetically stable complex on the same timescale. Although each cyclopentadienyl ring of $\mathbf{2c}^+$ has two sets of chemically nonequivalent protons, only a single broad signal centered at $\delta = 4.0$ ppm is detected for all the protons of the included cyclopentadienyl ligands (C_5H_4Et) of the guest. Unfortunately, at room temperature it was not possible to locate the signals arising from the protons of the ethyl groups of the bound guest. To study in more detail the dynamics of the inclusion complex $\mathbf{2c}^+$**@1**, we carried out VT ^{1}H NMR experiments in the range of 203–298 K and an EXSY experiment at 203 K on a sample containing **1** (1.16 mM) and $\mathbf{2c}^+$ (4.74 equiv; Figure 5). At 203 K the exchange rate between free and included $\mathbf{2c}^+$ is too slow to be detected by EXSY. However, at this temperature the broad signal resonating at $\delta \approx 4.0$ ppm at room temperature, which was assigned to the cyclopentadienyl protons of included $\mathbf{2c}^+$, splits into at least three separate signals.

This result indicates that at a low temperature the proton pairs of the cyclopentadienyl moieties become chemically nonequivalent. In the EXSY experiment carried out at 203 K we observed that the signals of the cyclopentadienyl

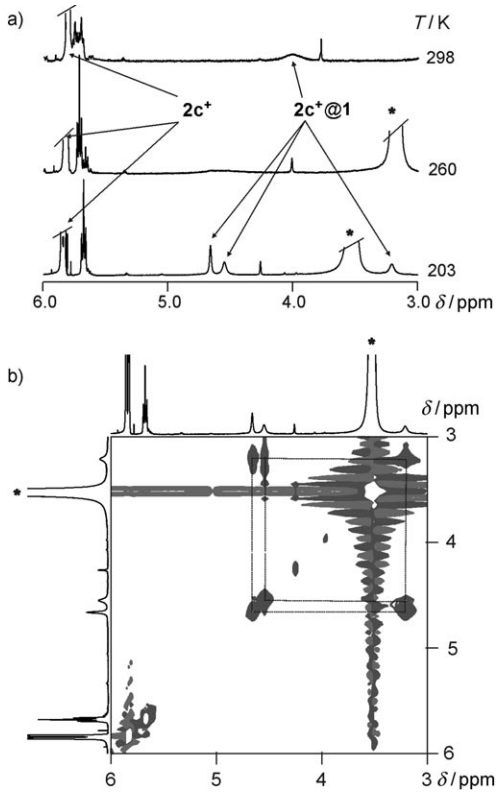

Figure 5. a) Observed changes in the proton signals of the cyclopentadienyl (C_5H_4Et) ligands for the $\mathbf{2c^+}$@**1** complex during a VT ^{1}H NMR experiment (from RT to 203 K) ([**1**] = 1.16 mM and [$\mathbf{2c^+}$] = 5.5 mM in [D_6]acetone). b) Expanded region of an EXSY experiment (6.00–3.00 ppm) performed at 203 K with the same sample (mixing time = 0.3 s). * indicates residual water from the deuteriated solvent.

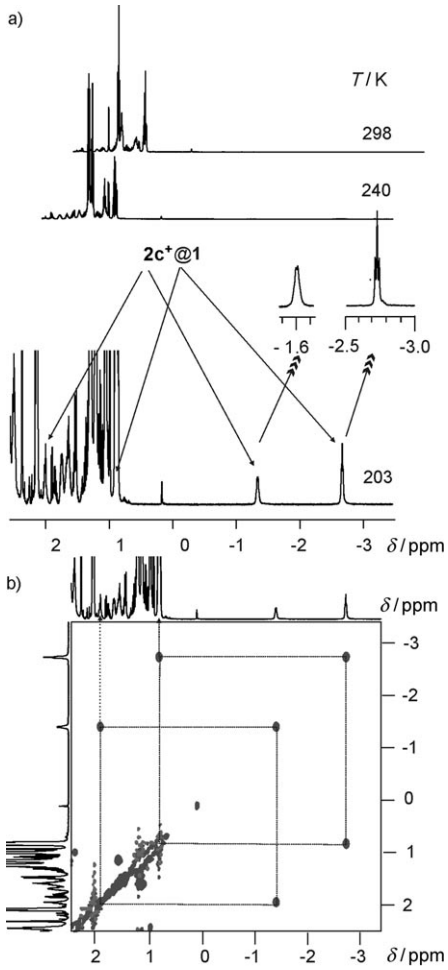

Figure 6. a) Observed changes in the upfield region of the ^{1}H NMR spectra of the $\mathbf{2c^+}$@**1** complex during a VT ^{1}H NMR experiment (from RT to 203 K; [**1**] = 1.16 mM) and [$\mathbf{2c^+}$] = 5.5 mM in [D_6]acetone). b) Expansion of the upfield region of an EXSY experiment (−3.00 to 2.50 ppm) performed at 203 K with the same sample (mixing time = 0.3 s).

protons resonating at $\delta = 4.7$ and 4.5 ppm were in chemical exchange with a broad signal centered at $\delta = 3.2$ ppm (Figure 5b). Furthermore, at this low temperature we also observed two signals at high field that arise from the methylene and methyl protons of one of the two ethyl substituents of included $\mathbf{2c^+}$ (Figure 6). The chemical shifts observed for this ethyl group ($\delta(CH_2) = -1.3$ and $\delta(CH_3) = -2.7$ ppm) place the residue deep inside the cavity of **1**. The EXSY experiment showed that this ethyl group is in slow chemical exchange with another ethyl substituent (Figure 6b). The chemical shifts of this second ethyl group ($\delta(CH_2) = 2.0$ and $\delta(CH_3) = 0.9$ ppm) are only slightly upfield-shifted relative to the shifts of free $\mathbf{2c^+}$. Taken together, these results indicate that metallocene $\mathbf{2c^+}$ is included in cavitand **1** with an equatorial geometry. The two ethyl groups of included metallocene $\mathbf{2c^+}$ adopt a *trans* conformation. One of the ethyl substituents of $\mathbf{2c^+}$ is included deep inside the cavitand, whereas the other is directed towards the open end of the structure (Figure 7). At 203 K the motion (tumbling) of the included guest, which is responsible for the chemical exchange between the two ethyl substituents, is slow on the ^{1}H NMR spectroscopy timescale. Thus, the protons of the two ethyl substituents of the cyclopentadienyl ligands of $\mathbf{2c^+}$ become chemically nonequivalent as a result of the inclusion process and the anisotropic magnetic shielding properties of **1**.

Generally, spinning of the guest along the C_4 axis of resorcinarene-based hosts is fast on the ^{1}H NMR spectroscopy timescale, but the tumbling motions of the guest that occur perpendicular to this axis can be slow.[16] We calculated the rate constant for the tumbling rotational motion of $\mathbf{2c^+}$ in **1** (by integration of the cross peaks and the diagonal peaks of the signals of the ethyl group) to be $k_1 = k_{-1} = 6.70\ s^{-1}$, which corresponds to a free energy barrier of $\Delta G^{\neq} = 10.95$ kcal mol^{-1}. The presence of the ethyl substituents in $\mathbf{2c^+}$ reduces the rate of tumbling compared with the unsubstituted guest $\mathbf{2a^+}$, for which we were unable to freeze out the fast rotational motion of the guest inside the host on the ^{1}H NMR spectroscopy timescale.

DFT-based calculations yielded three different geometries as energy minima for the $\mathbf{2c^+}$@**1** complex (Figure 7). In all the geometries, the central metal atom of the guest is not located as deeply inside cavitand **1** as observed for the non-substituted guests $\mathbf{2a^+}$ and $\mathbf{2b^+}$. In line with the ^{1}H NMR

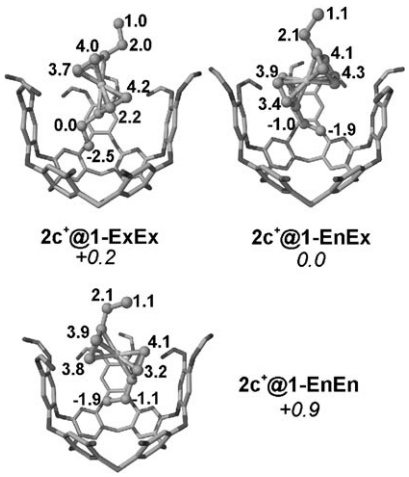

Figure 7. Optimized geometries for the inclusion complexes of 1,1′-diethylcobaltocenium guest $\mathbf{2c}^+$ in host **1**. All of the hydrogen atoms and one wall of the cavitand have been removed for clarity. The calculated chemical shifts of the guest's hydrogen atoms inside the host, relative to TMS, are shown in bold. The values in italics beneath each structure denote the energy of the complex in kcal mol^{-1} relative to the lowest-energy isomer. En and Ex refers to the relative *endo* or *exo* orientation of the methyl groups of $\mathbf{2c}^+$ with respect to the metallic center.

data, the calculations predict that $\mathbf{2c}^+$ preferentially adopts a pseudoequatorial orientation inside host **1** with one of the ethyl moieties of the guest located deep inside the cavitand. For the nonsubstituted guest $\mathbf{2a}^+$ we showed that the metallocenium guest can easily adopt two different extreme geometries (axial/equatorial) without significant loss of bonding energy with the host. The preferred orientation of the substituted guest $\mathbf{2c}^+$ inside host **1**, therefore, seems to be mainly governed by the steric requirements of the guest inside the host. Clearly, purely axial and/or equatorial orientations of the guest inside the host, as observed for guests $\mathbf{2a}^+$ and $\mathbf{2b}^+$, would lead to significant steric repulsion between the ethyl substituents of the guest and the walls of this host. This steric argument is also in line with the experimentally observed slower tumbling rate of guest $\mathbf{2c}^+$ in host **1** in comparison with cobaltocenium guest $\mathbf{2a}^+$ because this tumbling motion would require the formation of sterically congested axial and equatorial structures.

The three structures in Figure 7 have very similar energies and mainly differ in the orientations of the two ethyl moieties of guest $\mathbf{2c}^+$. All three are probably present in solution and interconvert rapidly by rotation of the two alkyl moieties around the cyclopentadienyl–CH_2 bond. From the energetic data depicted in Figure 7, average ^{1}H NMR chemical shifts for the protons of the guest inside host **1** at 200 K were calculated (assuming slow rotational motion of the guest on the ^{1}H NMR spectroscopy timescale). The calculations predict average values of $\delta = -2.1$ and -0.7 ppm for the CH_3 and CH_2 groups of the ethyl substituent of the guest that is included deeper inside the cavitand. These values are in moderate agreement with the experimentally observed values of $\delta = -2.7$ and -1.7 ppm. In addition, the values of $\delta = 1.1$ and 2.1 ppm calculated for the CH_3 and CH_2 groups of the ethyl substituent located at the open end of the cavitand reproduce much better the experimental values of $\delta = 0.8$ and 1.9 ppm. Also, the average chemical shift predicted for the protons of the cyclopentadienyl moiety deep inside the cavitand is $\delta = 3.3$ ppm and compares favorably with the experimental value of $\delta = 3.2$ ppm.

The correlation between the experimentally determined and the theoretically calculated chemical shifts is least good for the protons in the upper cyclopentadienyl moiety. Although experimentally chemical shifts of $\delta = 4.5$ and 4.6 ppm were obtained for these protons, calculations predicted an average chemical shift of $\delta = 4.1$ ppm for all four protons. It should be borne in mind, however, that the model host we used in our calculations lacked the ethyl substituents of the upper-rim amide moieties. From the structures in Figure 7 it is clear that the incorporation of these alkyl moieties into the model would alter the microenvironment around the upper cyclopentadienyl moiety of the encapsulated guest for all three structures. In addition, calculations were performed in the gas phase and therefore do not describe the effect of solvent on the microenvironment of the protons of the guest. Although this effect will be small for deeply encapsulated protons, it will be more pronounced for protons that are accessible to solvent molecules. In particular, the deshielded protons of the metallocene cyclopentadienyl moieties will be highly sensitive to these environmental effects.

Cyclopentadienyl[1-methyl-4-(1-methylethyl)benzene]ruthenium guest $\mathbf{2d}^+$: The complexation of $\mathbf{2d}^+$ by host **1** was studied by ^{1}H NMR spectroscopy through the addition of incremental amounts of guest to a 2.90 mM solution of **1** in [D_6]acetone. At room temperature both the signals of the host and the guest are involved in a slow chemical exchange on the ^{1}H NMR spectroscopy timescale between the free and bound states. The association constant for the inclusion complex was simply determined from the relative areas of the signals of the aromatic and amide protons of the free and bound receptor (Figure 8). Similarly to the observations for the complexation of cobaltocenium-based guests $\mathbf{2a}^+$

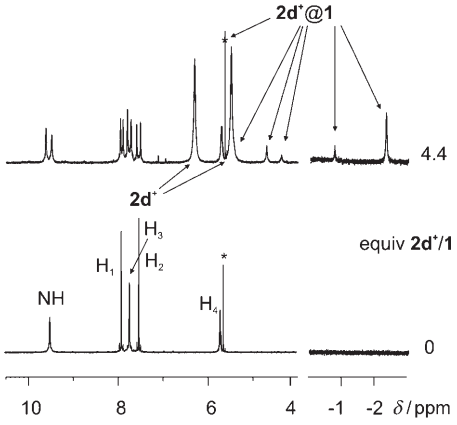

Figure 8. Changes in two regions of the ^{1}H NMR spectra acquired at 298 K (500 MHz, [D_6]acetone) during the titration of **1** with $\mathbf{2d}^+$. ([**1**] = 2.90 mM).

and $\mathbf{2c}^+$ to host **1**, the addition of substituents to the benzene moiety of guest $\mathbf{2b}^+$ led to a decrease in the stability constant of the resulting inclusion complex (Table 1). Surprisingly, the stability constants calculated for the inclusion complexes $\mathbf{2c}^+$@**1** and $\mathbf{2d}^+$@**1** are very similar, despite their very different substitution patterns (Table 1).

All the proton signals of the ruthenium guest $\mathbf{2d}^+$ shifted upfield upon inclusion within the cavity of host **1**. The largest upfield shifts were observed for the proton signals that correspond to the isopropyl substituent ($\Delta\delta = -3.6$ ppm for CH_3 and $\Delta\delta = -3.5$ ppm for CH) of the benzene ligand and for two aromatic protons of the benzene (C_6H_4) ligand ($\Delta\delta = -1.9$ ppm) of $\mathbf{2d}^+$. The complexation-induced chemical shift changes detected for the signals assigned to the cyclopentadienyl ligand protons ($\Delta\delta = -0.7$ ppm), to two other aromatic protons of the benzene moiety ($\Delta\delta = -0.8$ ppm), and to the methyl substituent of the benzene ligand ($\Delta\delta = -0.3$ ppm) are considerably smaller (Figures 9 and 10). These observations suggest that the benzene ligand and the isopropyl substituent penetrate deep inside the cavity, whereas the methyl and cyclopentadienyl moieties point towards the open end of the receptor cavitand **1**.

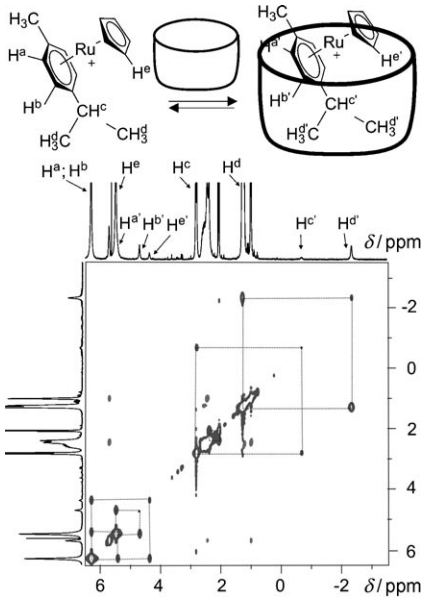

Figure 9. EXSY spectrum (500 MHz, [D_6]acetone) of **1** ([**1**] = 2.90 mM) containing 4.4 equivalents of $\mathbf{2d}^+$ at 298 K (mixing time 0.3 s).

We performed an EXSY experiment at room temperature on a 2.90 mM solution of cavitand **1** and 4.39 equiv of the cation $\mathbf{2d}^+$ to calculate the rate of self-exchange of the guest (Figure 9). We determined a rate constant of $k_{out} = 3.66\ s^{-1}$, which corresponds to a chemical exchange barrier of $\Delta G^{\neq}_{diss} = 16.67$ kcal mol^{-1} for the guest exiting the host. Clearly, decomplexation of included $\mathbf{2d}^+$ from host **1** occurs at a faster rate than the decomplexation of $\mathbf{2a}^+$ from the same host. Breaking down the energy barrier into its components as we did previously for complex $\mathbf{2a}^+$@**1** leads to a similar reorganization energy of the host ($\Delta G^{\neq}_{conf} = \Delta G^{\neq}_{diss} - \Delta G_{\mathbf{2a}+@\mathbf{1}} = 12.90$ kcal mol^{-1}). This suggests that conformational reorganization of the host to allow guest exchange should be very similar in the two complexes.

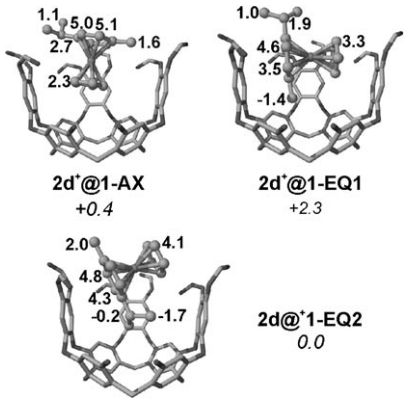

Figure 10. Optimized geometries for the inclusion complexes of guest $\mathbf{2d}^+$ with host **1**. All of the hydrogen atoms and one wall of the cavitand have been removed for clarity. The calculated chemical shifts of the guest hydrogen atoms inside the host, relative to TMS, are shown in bold. Values in italics beneath each structure denote the energy of the complex in kcal mol^{-1}, relative to the lowest energy isomer.

The optimized structures obtained for the nonsubstituted ruthenium system $\mathbf{2b}^+$@**1** were used as a starting point for the theoretical assessment of the geometries of the inclusion complex $\mathbf{2d}^+$@**1**. Addition of a methyl and an isopropyl group to the benzene moiety of $\mathbf{2b}^+$ yields two axial and two equatorial structures for the complexation of $\mathbf{2d}^+$ in host **1**. Optimization of these structures yielded the geometries, the calculated ^{1}H NMR chemical shifts, and the relative energies (Figure 10). We were unable to obtain a stable axial structure in which the *p*-cymene moiety is located inside the cavitand due to extensive steric repulsion between the bulky *p*-cymene group of the guest and the walls of host **1**.

In line with the ^{1}H NMR data, the lowest-energy structure is not the axial geometry $\mathbf{2d}^+$@**1-ax**, as was the case for the nonsubstituted guest $\mathbf{2b}^+$, but the pseudoequatorial geometry $\mathbf{2d}^+$@**1-eq2** in which the isopropyl group of the guest is located inside the cavitand. Although the calculated preference for this geometry over the axial geometry is very small, the experimental preference is probably considerably larger due to additional steric repulsion between the ethyl groups of the amide functions present in the upper rim of host **1** used for the experimental studies and the isopropyl and methyl moieties of the guest in the $\mathbf{2d}^+$@**1-ax** geometry. Moreover, solvophobic effects that may favor the inclusion of the aliphatic groups of $\mathbf{2d}^+$ inside the cavitand are not reproduced by these gas-phase calculations. In addition, the isopropyl group of the guest perfectly fills the cavity of host **1**, and consequently, conformation $\mathbf{2d}^+$@**1-eq2** will also be favored entropically over the other geometries.

The shortcomings in our theoretical model of the cavitand and the small energy differences between different orientations of the guest hampers an unambiguous determination

of the preferred complexation mode(s) of guest **2d** in host **1** based purely on the relative energies of the different structures shown in Figure 10. We can, however, compare the calculated ^{1}H NMR chemical shifts of the different structures of the complexes with the experimentally observed values. First, the large upfield shifts of the signals of both the CH_3 and CH protons of the isopropyl group of $\mathbf{2d}^+$ are only consistent with the values calculated for the isopropyl group in structure $\mathbf{2d}^+$@**1-eq2**. Secondly, the predicted large upfield shifts of the signals of the methyl moiety of $\mathbf{2d}^+$ in $\mathbf{2d}^+$@**1-eq1** and the cyclopentadienyl moiety of the guest in $\mathbf{2d}^+$@**1-ax** are not observed experimentally. Consequently, we conclude that structures $\mathbf{2d}^+$@**1-ax** and $\mathbf{2d}^+$@**1-eq1** are not present in solution in detectable concentrations and that the theoretical model, despite the aforementioned limitations, does reproduce the most favorable coordination mode of $\mathbf{2d}^+$ inside host **1** observed experimentally.

Similarly to what we discussed previously for the 1,1′diethyl-substituted cobaltocenium guest $\mathbf{2c}^+$, the chemical shifts calculated for the included aliphatic protons of guest $\mathbf{2d}^+$ are also in reasonable agreement with the experimental values. Larger discrepancies between the calculated and experimental chemical shifts are found for protons that are accessible to the solvent and/or are located in close proximity to the upper rim of the cavitand. The differences between the experimental and calculated ^{1}H NMR chemical shifts are more pronounced for this guest than for the previously studied complexes. We attribute this to the shallower inclusion of this guest inside **1** relative to the other guests. This is a result of the preferential inclusion of the large isopropyl group inside the cavitand, which makes the rest of the protons of guest $\mathbf{2d}^+$ more accessible to the solvent.

Conclusion

We have experimentally investigated the formation of kinetically and thermodynamically stable inclusion complexes of various transition-metal sandwich complexes with self-folding cavitand **1**. The rotational motions of the included metallocenes within cavitand **1** have also been studied. Small transition-metal guests, such as $\mathbf{2a}^+$ and $\mathbf{2b}^+$, tumble and spin freely inside **1**, easily interconverting between different complex geometries. The possible binding geometries of the inclusion complexes were investigated by electronic structure methods (DFT-based calculations). For small guests $\mathbf{2a}^+$ and $\mathbf{2b}^+$, DFT calculations predict a small preference for the formation of geometries in which the guest is complexed in an axial fashion. Equatorial complexation of the guest is not prohibitively high in energy, however, in line with the fast tumbling motion of these guests observed experimentally.

The presence of alkyl substituents in the aromatic ligands of the metallocene guests, as in $\mathbf{2c}^+$, reduces the rate of the tumbling motion of the guest inside the host's cavity. The cationic and asymmetric cyclopentadienyl(benzene)-ruthenium metallocene guest with a bulky isopropyl substituent on the benzene ligand, $\mathbf{2d}^+$, shows the preferential formation of a single binding geometry in which the isopropyl group is located deep inside the cavity. The guest inside the resulting inclusion complex does not display any sign of the tumbling motion. In addition, the alkyl substitution in guests $\mathbf{2c}^+$ and $\mathbf{2d}^+$ led to a considerable lowering of the stability constants of the corresponding inclusion complexes relative to those of the unsubstituted metallocenes, which demonstrates the strong size-selectivity of host **1**. The combined experimental and theoretical results presented herein provide an insight into the different complexation behavior of the different guests towards host **1**, as well as showing the effect of the shape and size of the guest on its dynamic motion inside the host.

Experimental Section

Synthesis: Complexes $\mathbf{2a}^+\cdot PF_6^-$, $\mathbf{2c}^+\cdot PF_6^-$, and $\mathbf{2d}^+\cdot PF_6^-$ were purchased from Sigma–Aldrich or ABCR Gmbh and used without further purification. Cavitand **1**[17] and the ruthenocenium guest $\mathbf{2b}^+\cdot Br^-$[18] were prepared as described in the literature. All solvents were of HPLC grade quality, obtained commercially, and used without further purification. Anhydrous solvents were collected from solvent purification system SPS-400-6 from Innovative Technologies. Flash column chromatography was performed on silica gel Scharlab60. ^{1}H NMR spectra were recorded either on a Bruker Avance DRX-400 or a DRX-500 spectrometer with residual nondeuteriated solvent as the internal standard.

^{1}H NMR titrations: All titrations were carried out on a Bruker 500 MHz spectrometer in [D_6]acetone by using solutions of octaamide host **1** at 298 K and adding aliquots of a solution of the relevant sandwich complex $\mathbf{2a}^+$–$\mathbf{2d}^+$ (in the same solvent), which was approximately 10 times more concentrated than the host solution. The concentration of receptor **1** was kept constant throughout the experiment. The association constants for the host–guest complex formed between octaamide host **1** and sandwich complexes **2** were simply determined from the relative areas of the ^{1}H NMR signals for free and bound **1**. The reported errors for the stability constants were estimated as the square root of the sum of the square of the standard deviation obtained from at least three experimental values of the binding constants determined in three experiments performed at different molar ratios of **1** to **2**.

EXSY experiments: The 2D NOESY spectra of solutions containing receptor **1** with an adequate molar excess of the corresponding guest ($\mathbf{2a}^+$–$\mathbf{2d}^+$) were recorded with the phase-sensitive NOESY pulse sequence supplied with the Bruker software. A mixing time of 300 ms and a 3 s relaxation delay between pulses was employed. The temperature of the probe was set at 298 K during the experiment with $\mathbf{2a}^+$, $\mathbf{2b}^+$, and $\mathbf{2d}^+$ and at 203 K for $\mathbf{2c}^+$. For each of the 512 F1 increments, 32 scans were accumulated. Before Fourier transformation, the FIDs were multiplied by a 90° sine-square function in both the F2 and F1 domains. 1K and 1K real data points were used in both dimensions. Integral values of the two-dimensional peaks were obtained from the spectra by using the Bruker processing software. The rate constants k_{in} and k_{out} were derived from the exchange intensity matrix based on the integration of a signal of the free and bound guest (cyclopentadienyl protons for $\mathbf{2a}^+$ and $\mathbf{2b}^+$, the ethyl group for $\mathbf{2c}^+$, and the isopropyl moiety for $\mathbf{2d}^+$) performed by using the ESXYCALC program (Mestreclab Research).[10,19]

Isothermal titration calorimetry (ITC) studies: ITC data were obtained on a VP-ITC MicroCalorimeter (MicroCal, LLC, Northampton, MA). The calorimetric titrations were performed by injecting 5 μL aliquots of a solution of cobaltocenium complex $\mathbf{2a}^+$ in acetone, approximately seven times more concentrated than the cavitand **1** ([**1**] = 6.6 mM, acetone) solution placed in the cell. After the reference titration had been subtracted, the association constant and the thermodynamic parameters were ob-

tained from the fit of the revised titration data to a theoretical titration curve by using the one set of sites model of the Microcal ITC Data Analysis module provided by MicroCal, LLC.

Electrochemical analysis: The cyclic voltammetry (CV) experiments were carried out by using an EC Epsilon Electrochemica Analyzer (C3-Cell Stand). A glassy carbon disk working electrode (0.071 cm^2), a platinum wire counter electrode, and a nonaqueous Ag/AgCl reference electrode were fitted to a single-compartment cell for the voltammetric experiments. The solutions were deoxygenated by purging with argon gas and maintained under an inert atmosphere for the duration of each electrochemical experiment. Stirring and gas-purging were carried out by remote control with a BASI PC-controlled potentiostat. A cyclic voltammogram was recorded after each addition.

Computational details: The choice of density functional theory to describe these supramolecular systems was not a trivial one. Indeed, it has been shown previously that most DFT methods fail to describe the dispersion-based interactions that are generally important in supramolecular chemistry. The predominant attractive interaction in the systems studied here, however, is not dispersion-based, but rather a cation–π interaction between the positively charged metallocenium guest and the electron-rich cavitand. This type of interaction is relatively well described by DFT-based methods. MP2 was considered as an alternative method, but the method seriously underestimated the cobalt–cyclopentadienyl distances in $CoCp_2^+$ compared with values obtained previously from crystal[20] and calculated[15] structures (see the Supporting Information). The use of higher correlated methods that more accurately describe weak dispersion-based interactions and that are also able to reproduce the structures of the sandwich complexes is not feasible due to the large size of the systems under study. Furthermore, ONIOM-type calculations, in which the overall computational cost is reduced by treating different parts of the system at different levels, cannot be applied here as the interaction between the host and guest involves the entire π system of the cavitand. For this reason, the host–guest complexes reported in this study were fully optimized at the DFT level. To reduce the computational cost, any alkyl chains located on the lower and/or upper rim of the host **1** were replaced by hydrogen atoms. Several DFT functionals were evaluated by a model system that consisted of a cobaltocenium cationic moiety sandwiched between two parallel benzene molecules (see the Supporting Information). The B97-1[21] functional reproduced the preferred orientation of the cobaltocenium between the two benzene moieties, and cobalt–benzene distances were determined at the MP2 and MP4//DFT levels of theory as well as the geometrical parameters of the metallocenium moiety in the crystal structure of $CoCp_2PF_6$.[20] This functional was consequently used in the rest of this study. Note that these observations are in line with previous benchmark studies that showed that the B97-1 functional performs well in describing systems containing nonbonding interactions.[22] All density functional theory based calculations were performed in Jaguar (version 6.5).[23] The calculations were performed by using the pseudospectral LACVP* basis set,[24] which consists of the 6-31G* basis set for nonmetal atoms and the Los Alamos effective core potentials and basis sets developed by Hay and Wadt for the metal atoms. Ultrafine integrals and an ultrafine DFT grid were employed throughout the calculations. The SCF energy convergence criterion was set to 1×10^{-8} a.u. and the RMS density matrix element change criterion was set to 1×10^{-6}. Default geometrical convergence criteria were used in the geometry optimization process for all the reported structures. Gas-phase NMR shielding constants were calculated by using the NMR module in the Jaguar program and values are reported relative to the shielding constants of tetramethylsilane, calculated at the same level of theory. Solvation effects on gas-phase optimized structures were evaluated by using a Poisson–Boltzmann implicit solvation model. Cyclohexane ($\varepsilon=2.023$, probe radius = 2.777 Å) and water ($\varepsilon=80.37$, probe radius = 1.400 Å) were chosen as model solvents.

Acknowledgements

We thank the Ministerio de Educación y Ciencia, SEUI for generous grants (Projects CTQ2005-08989-C01-C02/BQU, CTQ2005-0609-C02-02/BQU and Consolider Ingenio 2010 Grant CSD2006-0003). We also thank the ICIQ Foundation and the Generalitat de Catalunya DURSI (2005SGR00108, 2005SGR00715) for financial support. The Centre de Supercomputació de Catalunya (CESCA) is acknowledged for the use of their computational facilities.

[1] a) S. Mendoza, P. D. Davidov, A. E. Kaifer, *Chem. Eur. J.* **1998**, *4*, 864–870; b) A. E. Kaifer, *Acc. Chem. Res.* **1999**, *32*, 62–71; c) C. M. Cardona, S. Mendoza, A. E. Kaifer, *Chem. Soc. Rev.* **2000**, *29*, 37–42; d) W. Ong, A. E. Kaifer, *Organometallics* **2003**, *22*, 4181–4183; e) K. Moon, A. E. Kaifer, *J. Am. Chem. Soc.* **2004**, *126*, 15016–15017.

[2] a) A. V. Davis, D. Fiedler, G. Seeber, A. Zahl, R. Van Eldik, K. N. Raymond, *J. Am. Chem. Soc.* **2006**, *128*, 1324–1333; b) D. Fiedler, R. G. Bergman, K. N. Raymond, *Angew. Chem.* **2006**, *118*, 759–762; *Angew. Chem. Int. Ed.* **2006**, *45*, 745–748.

[3] a) V. F. Slagt, J. N. H. Reek, P. C. J. Kamer, P. W. N. M. Van Leeuwen, *Angew. Chem.* **2001**, *113*, 4401–4404; *Angew. Chem. Int. Ed.* **2001**, *40*, 4271–4274; b) D. Fiedler, D. H. Leung, R. G. Bergman, K. N. Raymond, *Acc. Chem. Res.* **2005**, *38*, 349–358; c) A. W. Kleij, J. N. H. Reek, *Chem. Eur. J.* **2006**, *12*, 4218–4227; d) T. S. Koblenz, H. L. Dekker, C. G. De Koster, P. W. N. M. Van Leeuwen, J. N. H. Reek, *Chem. Commun.* **2006**, 1700–1702; e) M. Kuil, T. Soltner, P. W. N. M. Van Leeuwen, J. N. H. Reek, *J. Am. Chem. Soc.* **2006**, *128*, 11344–11345; f) D. H. Leung, R. G. Bergman, K. N. Raymond, *J. Am. Chem. Soc.* **2006**, *128*, 9781–9797; g) D. H. Leung, R. G. Bergman, K. N. Raymond, *J. Am. Chem. Soc.* **2007**, *129*, 2746–2747.

[4] a) D. M. Rudkevich, G. Hilmersson, J. Rebek, Jr., *J. Am. Chem. Soc.* **1998**, *120*, 12216–12225; b) T. Haino, D. M. Rudkevich, A. Shivanyuk, K. Rissanen, J. Rebek, Jr., *Chem. Eur. J.* **2000**, *6*, 3797–3805.

[5] a) B. W. Purse, A. Gissot, J. Rebek, Jr., *J. Am. Chem. Soc.* **2005**, *127*, 11222–11223; b) S. M. Butterfield, J. Rebek, Jr., *Chem. Commun.* **2007**, 1605–1607; c) R. J. Hooley, J. Rebek, Jr., *Org. Biomol. Chem.* **2007**, *5*, 3631–3636.

[6] M. D. Pluth, K. N. Raymond, *Chem. Soc. Rev.* **2007**, *36*, 161–171.

[7] P. Ballester, M. A. Sarmentero, *Org. Lett.* **2006**, *8*, 3477–3480.

[8] M. A. Sarmentero, P. Ballester, *Org. Biomol. Chem.* **2007**, *5*, 3046–3054.

[9] a) D. M. Rudkevich, G. Hilmersson, J. Rebek, *J. Am. Chem. Soc.* **1997**, *119*, 9911–9912; b) A. D. M. Rudkevich, G. Hilmersson, J. Rebek, Jr., *J. Am. Chem. Soc.* **1998**, *120*, 12216–12225; c) A. Shivanyuk, K. Rissanen, S. K. Korner, D. M. Rudkevich, J. Rebek, Jr., *Helv. Chim. Acta* **2000**, *83*, 1778–1790.

[10] C. L. Perrin, T. J. Dwyer, *Chem. Rev.* **1990**, *90*, 935–967.

[11] a) R. Wyler, J. de Mendoza, J. Rebek, Jr., *Angew. Chem.* **1993**, *105*, 1820–1821; *Angew Chem. Int. Ed.* **1993**, *32*, 1699–1701; b) N. Branda, R. Wyler, J. Rebek, Jr., *Science* **1994**, *263*, 1267–1268; c) F. Hof, L. C. Palmer, J. Rebek, Jr., *J. Chem. Educ.* **2001**, *78*, 1519–1521.

[12] For related biding geometries proposed for the adducts of cyclodextrins and ferrocene, see: F. Hapiot, S. Tilloy, E. Monflier, *Chem. Rev.* **2006**, *106*, 767–781.

[13] T. Matsue, D. H. Evans, T. Osa, N. Kobayashi, *J. Am. Chem. Soc.* **1985**, *107*, 3411–3417.

[14] S. Mendoza, E. Castano, Y. Meas, L. A. Godinez, A. E. Kaifer, **2004**, *16*, 1469–1477.

[15] Z.-F. Xu, Y. Xie, W.-L. Feng, H. F. Schaefer III, *J. Phys. Chem. A* **2003**, *107*, 2716–2729.

[16] M. Pons, O. Millet, *Prog. Nucl. Magn. Reson. Spectrosc.* **2001**, *38*, 267–324.

[17] P. Ballester, A. Shivanyuk, A. R. Far, J. Rebek, Jr., *J. Am. Chem. Soc.* **2002**, *124*, 14014–14016.

[18] R. A. Zelonka, M. C. Baird, *J. Organomet. Chem.* **1972**, *44*, 383–389.

[19] Z. Zolnai, N. Juranic, D. Vikic-Topic, S. Macura, *J. Chem. Inf. Comput. Sci.* **2000**, *40*, 611–621.
[20] D. Braga, L. Scaccianoce, F. Grepioni, S. M. Draper, *Organometallics* **1996**, *15*, 4675–4677.
[21] F. A. Hamprecht, A. J. Cohen, D. J. Tozer, N. C. Handy, *J. Chem. Phys.* **1998**, *109*, 6264–6271.
[22] a) E. R. Johnson, R. A. Wolkow, G. A. DiLabio, *Chem. Phys. Lett.* **2004**, *394*, 334–338; b) Y. Zhao, D. G. Truhlar, *J. Phys. Chem. A* **2005**, *109*, 5656–5667; c) Y. Zhao, D. G. Truhlar, *J. Phys. Chem. A* **2006**, *110*, 5121–5129.
[23] Jaguar 6.5, Schrödinger, Portland, OR, **1991–2003**.
[24] P. J. Hay, W. R. Wadt, *J. Chem. Phys.* **1985**, *82*, 299–310.

Received: April 3, 2008
Published online: July 10, 2008

